American Mineralogist, Volume 75, pages 915–922, 1990

Baumhauerite-*2a*: A silver-bearing mineral with a baumhauerite-like supercell from Lengenbach, Switzerland

Allan Pring
South Australian Museum, North Terrace, Adelaide, South Australia, 5000, Australia
William D. Birch
Museum of Victoria, 285 Russell Street, Melbourne, Victoria, 3000, Australia
David Sewell
Department of Geology, University of Melbourne, Parkville, Victoria, 3052, Australia
Stefan Graeser
Natural History Museum, CH 4001 Basel, Switzerland and Mineralogical Institute, University of Basel, CH 4056, Switzerland
Andreas Edenharter
Mineralogisch-Kristallographisches Institut, Universität Göttingen, V.M. Goldschmidt Str. 1, D-3400 Göttingen, Federal Republic of Germany
Alan Criddle
Department of Mineralogy, British Museum (Natural History), Cromwell Road, London SW7 5BD, England

Abstract

Baumhauerite-*2a* is a silver-bearing mineral having a superstructure derived from a baumhauerite-like structure, with an average composition $Pb_{11}Ag_{0.7}As_{17.2}Sb_{0.4}S_{36}$. Baumhauerite-*2a* occurs as an intergrowth with a silver-free baumhauerite in dolomite at Lengenbach, Binntal, Valais, Switzerland. Baumhauerite-*2a* is massive, opaque, and steel gray with a metallic luster and a dark reddish brown streak. Baumhauerite-*2a* has one perfect cleavage on (100), has a conchoidal fracture, and is brittle. The microhardness VHN_{50} is 156–165, mean 159, corresponding to a Mohs hardness of 3. In reflected plane-polarized light, the mineral varies in color from white to off white; the mineral is bireflectant and nonpleochroic. Reflectance values are tabulated and compared with those of baumhauerite. Powder X-ray diffraction data were indexed on a monoclinic cell having $a = 44.74(4)$, $b = 8.477(4)$, $c = 7.910(6)$ Å, $\beta = 93.37°(5)$ and $Z = 2$. Strongest reflections in the powder diffraction pattern [*d* in Å (*I*) *hkl*] 4.22, (80), 120; 3.68, (60), 911, 221; 3.21, (60), $\bar{1}3.0.1$; 3.01, (100), 13.1.1; 2.95, (70), 921; 2.75, (90), 11.0.2; 2.73, (70), $\bar{6}22$; 2.28, (90), $\bar{3}32$. The mineral's superstructure is believed to be due to the ordering of Pb, Ag, or As atoms over two baumhauerite-like cells. High-resolution lattice images show that baumhauerite-*2a* and baumhauerite can intergrow at the unit cell level. The mineral is named for its relationship to baumhauerite.

Introduction

Lengenbach, Binntal, Canton Valais, Switzerland, is well known for the occurrence of rare sulfosalt minerals, particularly the Pb-As sulfides, many of which have not been found elsewhere. The sulfosalts occur with pyrite and realgar in cavities in a Triassic dolomite that lies at the outer edge of the Monte-Leone Nappe (Graeser, 1965, 1977). Six well-characterized Pb-As sulfide minerals have been identified from the deposit: sartorite, rathite, baumhauerite, liveingite, dufrenoysite, and jordanite. With the exception of jordanite, these minerals are chemically and structurally very closely related, having two unit-cell repeats, 8.4 Å and 7.9 Å, in common (Makovicky, 1985). In addition to these well-characterized phases, a number of poorly defined phases have also been reported, most of which appear to be superstructures of the better-defined species. The nature of supercell formation in these minerals is poorly understood, and there is a lack of accurate chemical and X-ray data for most of them. Physically and optically they are very similar to their parent phases.

We have undertaken a systematic study of the lead-arsenic sulfide minerals with powder X-ray diffraction, electron microprobe analyses and high-resolution transmission electron microscopy (HRTEM) techniques in order to characterize these supercell phases and to try to establish the nature of supercell ordering. In this paper we will confine ourselves to baumhauerite and the closely related new mineral baumhauerite-*2a*. The mineral and name, baumhauerite-*2a*, were approved by the Commis-

0003–004X/90/0708–0915$02.00

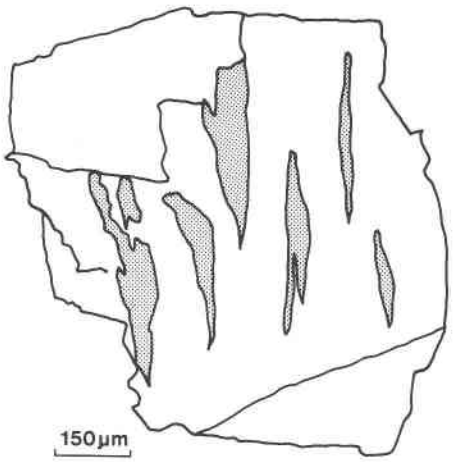

Fig. 1. Sketch showing the textural relationship between baumhauerite-*2a* and baumhauerite in a massive intergrowth.

Table 1. *R* and ^{im}R values for baumhauerite-*2a* and baumhauerite (specimen M3010)

	Baumhauerite-*2a*				Baumhauerite			
nm	R_1	R_2	$^{im}R_1$	$^{im}R_2$	R_1	R_2	$^{im}R_1$	$^{im}R_2$
400	38.9	41.9	23.2	26.6	38.0	42.1	22.4	26.7
420	38.4	41.6	22.6	26.0	37.6	41.9	21.95	26.2
440	37.85	41.3	22.05	25.5	37.2	41.6	21.55	25.7
460	37.3	40.9	21.4	25.0	36.8	41.2	21.1	25.3
470	37.1	40.7	21.2	24.8	36.6	41.0	20.9	25.05
480	36.85	40.5	20.9	24.6	36.4	40.7	20.7	24.8
500	36.2	40.2	20.3	24.2	36.0	40.4	20.2	24.3
520	35.6	39.6	19.7	23.65	35.5	39.8	19.8	23.8
540	34.9	39.0	19.1	23.0	35.1	39.2	19.4	23.2
546	34.7	38.7	18.9	22.7	35.0	39.05	19.3	23.0
560	34.15	38.1	18.5	22.2	34.6	38.6	18.9	22.5
580	33.5	37.3	17.9	21.5	34.2	37.9	18.5	21.9
589	33.1	36.9	17.6	21.1	33.9	37.5	18.3	21.6
600	32.8	36.4	17.3	20.65	33.7	37.2	18.1	21.3
620	32.1	35.6	16.7	19.9	33.2	36.5	17.6	20.6
640	31.35	34.7	16.1	19.2	32.5	35.7	17.0	19.9
650	31.05	34.4	15.9	18.9	32.2	34.3	16.7	19.6
660	30.6	34.0	15.6	18.4	31.8	34.9	16.4	19.3
680	30.1	33.3	15.0	17.8	31.1	34.2	15.8	18.6
700	29.6	32.65	14.65	17.3	30.5	33.5	15.3	18.0

sion on New Minerals and Mineral Names, I.M.A., in 1989.

Sample description

A number of specimens containing baumhauerite-*2a* and baumhauerite were examined. Specimens M3010 and M30980 from the Museum of Victoria and BM 1926 1654 from the British Museum (Natural History) are massive and contain a heterogeneous intergrowth of baumhauerite-*2a* and baumhauerite. Three additional specimens examined, L7228, L9501, and L15621, from the collection of the Naturhistorisches Museum, Basel, are composed of pure baumhauerite-*2a*. Specimens M3010, BM 1926 1654 and L7228 are designated as being cotypes of baumhauerite-*2a*; several fragments from specimen M3010 are also preserved in the collection of the South Australian Museum (Catalogue number G 15547). All of the specimens were from the quarry at Lengenbach, Binntal, Switzerland. The exact locality within the quarry is unknown, but the mineral may be fairly widespread.

Optical and physical properties

The physical and optical properties of baumhauerite-*2a* and baumhauerite differ only subtly, and the two minerals are difficult to distinguish without recourse to powder X-ray diffraction methods. In hand specimen, both minerals are opaque and steel gray with a metallic luster. The streak is dark reddish brown. The minerals are brittle with a conchoidal fracture, and baumhauerite-*2a* has one perfect cleavage, probably on (100), similar to that of baumhauerite. It was not possible to measure the density of baumhauerite-*2a* owing to the nature of the intergrowth of baumhauerite-*2a* and baumhauerite, but the calculated density is 5.31 g/cm^3.

The mineral has a Mohs hardness of 3 and a microhardness VHN_{50} in the range 156–165, with an average of 159 based on 5 indentations. The microhardness of the baumhauerite associated with baumhauerite-*2a* is somewhat higher, being in the range 177–184 with an average of 181 based on seven indentations.

The reflected light properties of baumhauerite-*2a* were determined on fragments from specimen M3010, which contained an intergrowth of baumhauerite-*2a* and baumhauerite. The specimen was polished for examination using the procedures as described by Criddle et al. (1983). In plane polarized light, baumhauerite-*2a* and baumhauerite are indistinguishable, varying in color from white to off white; both minerals are moderately anisotropic with subtly different rotation tints; from extinction the sequence for baumhauerite-*2a* is brownish gray, greenish gray, very pale bluish gray and pale greenish gray; those of the accompanying baumhauerite are dark brown, light brown and light brownish gray. The differences in tints between the minerals are subtle, and although it is possible to distinguish one mineral from the other when both are present, if only one were present, the best that could be hoped for was that one could say that it could be baumhauerite or baumhauerite-*2a*.

In the specimen examined, baumhauerite is characterized by fine lamellar twinning, which is absent from baumhauerite-*2a*. The latter occurs within baumhauerite as lenses, some of which are flamelike in shape and others arcuate and sigmoidal (Fig. 1). The red internal reflections common in baumhauerite were not observed in baumhauerite-*2a*.

Reflectance measurements were made using the procedures and equipment described by Criddle (in Cabri et al., 1981), except that air and oil 16× objectives were used. The effective numerical apertures of these objectives were adjusted to 0.15 by means of the illuminator aperture diaphragm.

Four areas were measured: two of baumhauerite and two of baumhauerite-*2a*. The reflectance spectra (Fig. 2)

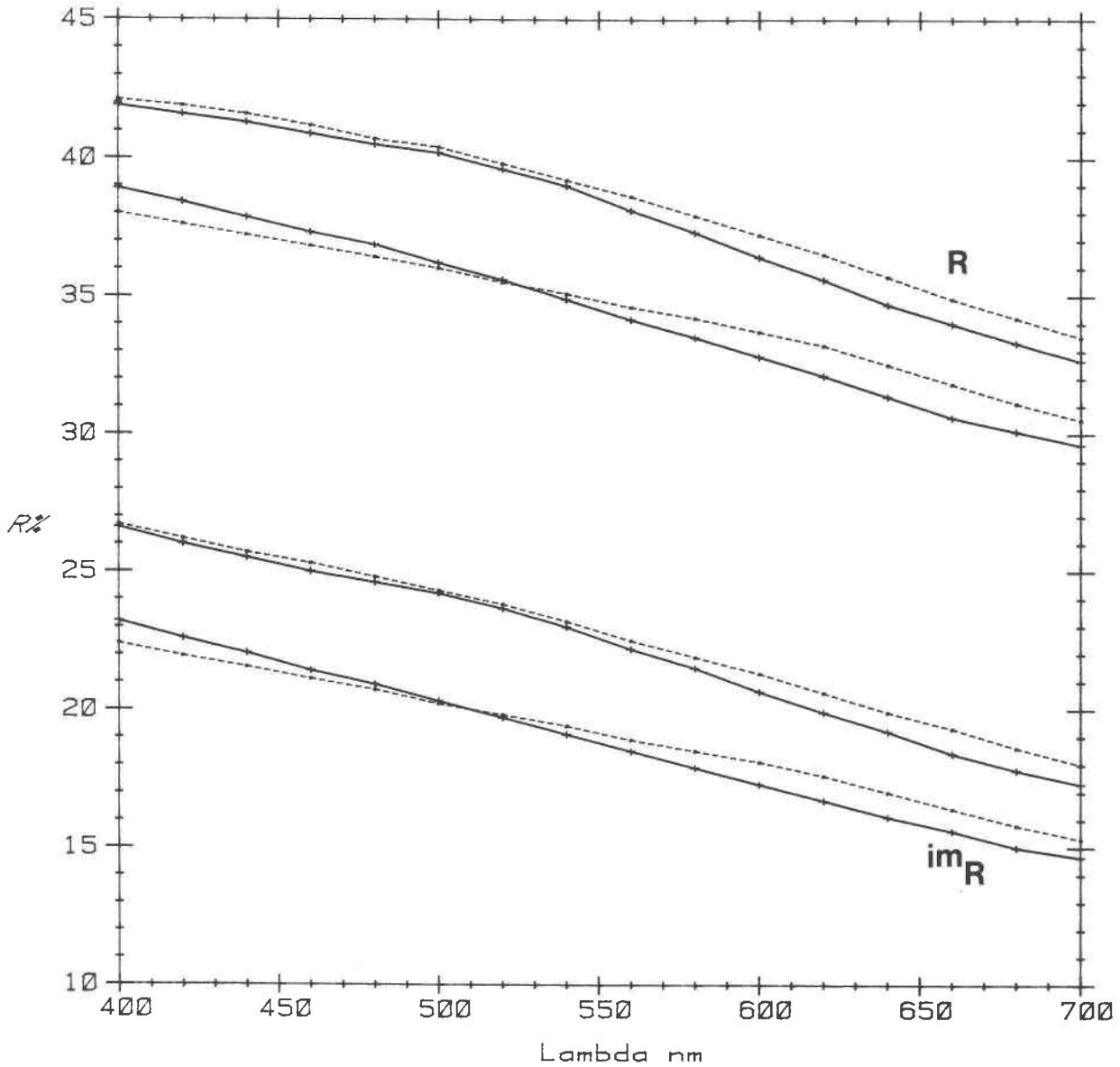

Fig. 2. R_1, R_2 and $^{im}R_1$, $^{im}R_2$ spectra for baumhauerite (dashed lines) and baumhauerite-*2a*.

confirm the visual impression that the two minerals are optically very similar, but it is clear that there are slight differences in the dispersion of their reflectances, as there should be, if the rotation tints differ. Data for two of the measured areas are summarized in Table 1. These results are consistently lower than those of the baumhauerite reported by Picot and Johan (1982), and the dispersion of their reflectance spectra match much more closely those of baumhauerite-*2a* than baumhauerite. It is worth recalling that some samples from Binntal consist entirely of baumhauerite-*2a* and that the distinction between baumhauerite and baumhauerite-*2a* was unknown to Picot and Johan (1982).

Although great care was taken to obtain a perfect specular surface for our measurements, some of our data are in error (by as much as 0.1% absolute). Both baumhauerite-*2a* and baumhauerite are essentially transparent in the orange-to-red region of the visible spectrum, and it is in this region that our R and ^{im}R data produce erroneous absorption coefficients (cf. Embrey and Criddle, 1978). Given this fact, it may well be that, in larger, less well-polished samples, or on fractured surfaces, baumhauerite-*2a* will also display red internal reflections.

Chemistry

Quantitative electron microprobe analyses of baumhauerite-*2a* and the associated baumhauerite were initially obtained using the electron microprobes at the De-

Table 2. Summary of baumhauerite-*2a* and baumhauerite compositional data

Elements	Baumhauerite				Baumhauerite-*2a*					
	BM 1926,1654		M3010		BM 1926,1654		M3010		L7228	
	1.	2.	1.	2.	1.	2.	1.	2.	1.*	2.
					Wt%					
Pb	48.3	47.5	52.8	51.3	48.2	47.1	48.1	46.2	46.2	46.3
Ag	—	—	0.1	—	1.5	1.4	1.6	1.6	1.4	1.4
Tl	n.d.	0.8	n.d.	0.4	n.d.	0.5	n.d.	0.8	—	—
As	26.5	27.9	24.1	25.1	25.5	26.8	25.9	27.4	26.3	26.9
Sb	1.2	—	0.6	—	1.1	—	0.8	—	0.5	0.5
S	23.2	24.6	21.9	23.1	22.6	23.9	22.6	24.2	25.6	24.3
Total	99.2	100.8	99.5	99.9	98.9	99.7	99.0	100.2	100.0	99.4
					Atomic proportions					
Pb	11.6	10.7	13.5	12.4	11.9	10.9	11.8	10.6	10.0	10.8
Ag	—	—	—	—	0.7	0.6	0.8	0.7	0.6	0.6
Tl	—	0.2	—	0.1	—	0.1	—	0.2	—	0.2
As	17.6	17.4	17.0	16.7	17.4	17.3	17.6	17.4	15.8	17.3
S	36	36	36	36	36	36	36	36	36	36

Note: n.d. = not detected. Analyses 1. University of Melbourne, W. D. Birch and D. Sewell analysts. Analysis 1*. E.T.H. Zurich, A. Edenharter analyst. Analyses 2. University of Göttingen, A. Edenharter analyst.

partment of Geology, University of Melbourne (M3010 and BM 1926 1654) and at Eidgenössische Technische Hochschule, Zurich (L 7228). A duplicate set of analyses was undertaken at the University of Göttingen to confirm the significant variation in composition of the specimens. Analytical standards used in Melbourne were galena (Pb), arsenopyrite (As,S), pure Sb, and pure Ag. The specimen current ranged from 0.015 μA to 0.025 μA with an accelerating voltage of 20 kV. Analyses at Zurich and Göttingen used the following standards galena (Pb), stibnite (Sb and S), synthetic lorandite (Tl and As), and synthetic pyrargyrite (Ag), with an accelerating voltage of 15 kV and a specimen current of about 8 ηA. The analyses of the specimens examined are presented in Table 2. The compositions within samples fall into two distinct groups: Ag-free compositions defined as having Ag < 0.2% and compositions having Ag ~ 1.5%. Intermediate compositions were not found, suggesting that there are two compositionally distinct phases rather than a single phase that is compositionally zoned. This conclusion is confirmed optically. Energy-dispersive X-ray analyses (EDA) and electron diffraction examination revealed that the higher Ag contents are associated with baumhauerite-*2a* and the accompanying baumhauerite is essentially Ag-free.

The electron microprobe analyses gave the average formula (the mean of three specimens, both sets of analyses calculated on the basis of 36 S atoms) $Pb_{11}Ag_{0.7}As_{17.2}Sb_{0.4}S_{36}$ for baumhauerite-*2a* and $Pb_{12}As_{17.2}S_{36}$ for baumhauerite. The compositional relations suggest that Ag would replace As. The analyses show a range of compositions for baumhauerite-*2a*, with the duplication of the analyses at the University of Göttingen confirming that these differences are real and not wholly associated with problems in the ZAF correction procedures for the analyses. The two sets of analyses are in good agreement, but they also illustrate the dramatic effect that small errors in S analyses have on the stoichiometry of the formula.

X-ray diffraction data

Precession and Weissenberg single-crystal X-ray photographs were obtained using a small fragment of baumhauerite-*2a* from specimen L7228. These photographs showed that baumhauerite-*2a* has a monoclinic unit cell with $a = 44.41(1)$, $b = 8.49(2)$, $c = 7.92(1)$ Å, and $\beta = 93°41'$.

The powder X-ray diffraction pattern of baumhauerite-*2a* was recorded using a Guinier-Hägg camera (100-mm diameter) with monochromated Cu$K\alpha$ radiation and silicon as an internal standard. The powder pattern contains some lines from baumhauerite, as the intimacy of the intergrowth between the two forms of baumhauerite prevents their separation. The pattern also contains a number of lines from jordanite. The powder diffraction data for baumhauerite-*2a* are given in Table 3; lines due to jordanite and baumhauerite have been omitted.

As they are chemically and physically similar, powder X-ray diffraction offers the simplest method to differentiate between the two forms of baumhauerite. The pattern of baumhauerite-*2a* was indexed on a monoclinic cell with the aid of single-crystal photographs and refined by least-squares methods using 54 reflections with $2\theta < 40°$. The following cell parameters were obtained: $a = 44.74(4)$, $b = 8.477(4)$, $c = 7.910(6)$ Å, and $\beta = 93.37°(5)$. X-ray diffraction data were recorded for three specimens of baumhauerite-*2a*, and only minor variations in cell dimensions were found (Table 4). Comparison with the triclinic cell of baumhauerite—$a = 22.80$, $b = 8.357$, $c = 7.89$ Å, $\alpha = 90°03'$, $\beta = 97°16'$, $\gamma = 89°55'$ (Engel and Nowacki, 1969)—shows that the two phases are closely related, but the a repeat is not simply twice that of baumhauerite, as the doubling of a permits the choice of a slightly different reduced cell. The powder data can also be indexed on an alternate monoclinic cell with $a = 45.7(4)$, $b = 8.39(4)$, $c = 7.87(3)$ Å, and $\beta = 97.08'(6)$.

TABLE 3. Powder X-ray diffraction data for baumhauerite-*2a* BM 1926 1654

I_{obs}*	d_{obs}, Å	d_{cal}, Å	*hkl*
20	11.11	11.171	400
5	8.49	8.476	010
10	7.72	7.697	101
5	7.38	7.367	310
20	7.16	7.151	$\bar{3}01$
5	6.40	6.383	700
10	6.16	6.150	510
10	6.09	6.096	$\bar{5}01$
10	5.84	5.777	$01\bar{1}$ (?)
10	5.73	5.751	501
5	5.59	5.594	610
10	4.80	4.827	701
80	4.22	4.219	120
40	4.16	4.164	220
10	3.95	3.947	002
30	3.87	3.872	$\bar{3}02$
40	3.79	3.792	$\bar{4}02$
60	3.68	3.683	911
		3.665	221
50	3.65	3.655	402
20	3.60	3.599	321
10	3.57	3.571	$\bar{4}21$
30	3.50	3.504	212
30	3.47	3.480	$\bar{5}21$
30	3.46	3.462	$\bar{4}12$
20	3.41	3.409	12.1.0
		3.406	602
20	3.39	3.392	$\bar{1}1.1.1$
10	3.36	3.356	412
10	3.31	3.316	$\bar{8}02$
60	3.21	3.221	$\bar{1}3.0.1$
5	3.14	3.138	802
5	3.07	3.070	12.1.1
		3.065	821
10	3.05	3.054	712
100	3.01	3.011	$\bar{1}3.1.1$
70	2.95	2.945	921
40	2.93	2.932	11.2.0
50	2.90	2.905	$\bar{1}0.2.1$
20	2.89	2.890	$\bar{1}22$
		2.889	022
30	2.82	2.820	130
20	2.78	2.776	330
20	2.77	2.768	422
90	2.75	2.752	11.0.2
70	2.73	2.733	$\bar{6}22$
20	2.71	2.713	11.2.1
50	2.65	2.652	16.1.0
10	2.64	2.641	630
20	2.63	2.628	$\bar{3}31$
20	2.61	2.610	331
20	2.56	2.563	$\bar{5}31$
20	2.42	2.423	413
20	2.38	2.380	10.2.2
30	2.34	2.342	613
20	2.33	2.325	931
90	2.28	2.282	$\bar{3}32$
30	2.26	2.261	$\bar{1}6.1.2$

Note: Cell $a = 44.74(4)$, $b = 8.477(4)$, $c = 7.910(6)$ Å, $\beta = 93.37°(5)$.
* Intensities estimated visually.

This is clearly a *2a* supercell of baumhauerite, although the reflection at d = 11.11 Å, which is sometimes absent, cannot be indexed with the cell with $a = 45.7$ Å. Baumhauerite-*2a* may also be triclinic, but, if so, the deviations of α and γ from 90° are very small, and the uncertainties in assigning indices to higher angle reflections prevent accurate refinement of a triclinic cell.

TABLE 4. Cell parameters for baumhauerite-*2a*

Specimen no.	*a* Å	*b* Å	*c* Å	β
BM(MH) 1926 1654	44.74(4)	8.477(4)	7.910(6)	93.37°(5)
M3010	44.2(1)	8.45(4)	7.91(3)	93.6°(2)
L7228	44.25(6)	8.497(11)	7.934(10)	93.9°(2)
L7228*	44.41(1)	8.49(2)	7.92(1)	93.68°

* From single-crystal photographs.

ELECTRON MICROSCOPY

Samples were prepared for the electron microscope by grinding in acetone and by depositing a drop of the resulting suspension onto holey carbon films. These fragments were examined at a magnification of 360 000× in a modified JEM-200CX electron microscope fitted with a top-entry goniometer and an energy-dispersive X-ray detector. The characteristics of the objective lens at 200 kV are $C_s = 1.9$ mm and $C_c = 1.9$ mm, giving a point-to-point resolution of approximately 2.5 Å at the so-called Scherzer focus (Scherzer, 1949).

Figures 3a and 3b shows electron diffraction patterns for baumhauerite and baumhauerite-*2a*, projected down [001]. The doubling of the *a* cell repeat is apparent when the two diffraction patterns are compared. The distribution of the strong subcell reflections is common to both patterns, indicating that the structures of the two minerals are composed of the same basic subcell units.

High-resolution lattice images of baumhauerite and baumhauerite-*2a* confirm the close relationship between the two phases (Figs. 4a and 4b). The baumhauerite image shows that the *a* repeat is composed of two distinct lattice motifs (Fig. 4a), whereas four motifs are visible along the *a* repeat of baumhauerite-*2a* (Fig. 4b). The doubling of the *a* repeat can be seen by comparison of Figures 4a and 4b; the 8.4-Å repeat along [010] is the same in both images. Baumhauerite and baumhauerite-*2a* clearly have a common structural framework, i.e., the order of the structural units is the same in both phases, and the structure repeats differ, probably because of cation ordering. The details of the lattice motifs in the two images are similar but not identical. This is not unexpected, as the structures not only contain slightly different cation-ordering schemes, but the images also were recorded at different objective lens defocus values. Within an image the effects of thickness on lattice motifs can be great; for example, in Figures 4a and 4b, crystal thickness decreases from the top of the image to the bottom. The doubled-cell repeat of baumhauerite-*2a* is distinct in regions of intermediate thickness (~100 Å). At greater thickness and in very thin regions the contrast differences among the four layers in the doubled cell are much less distinct.

Figure 5 shows an irregular intergrowth of the two forms; baumhauerite-*2a* is the dominant phase with small strips of baumhauerite intergrown. The intergrowth of the two minerals at the unit-cell level indicates that the structural difference between baumhauerite and baum-

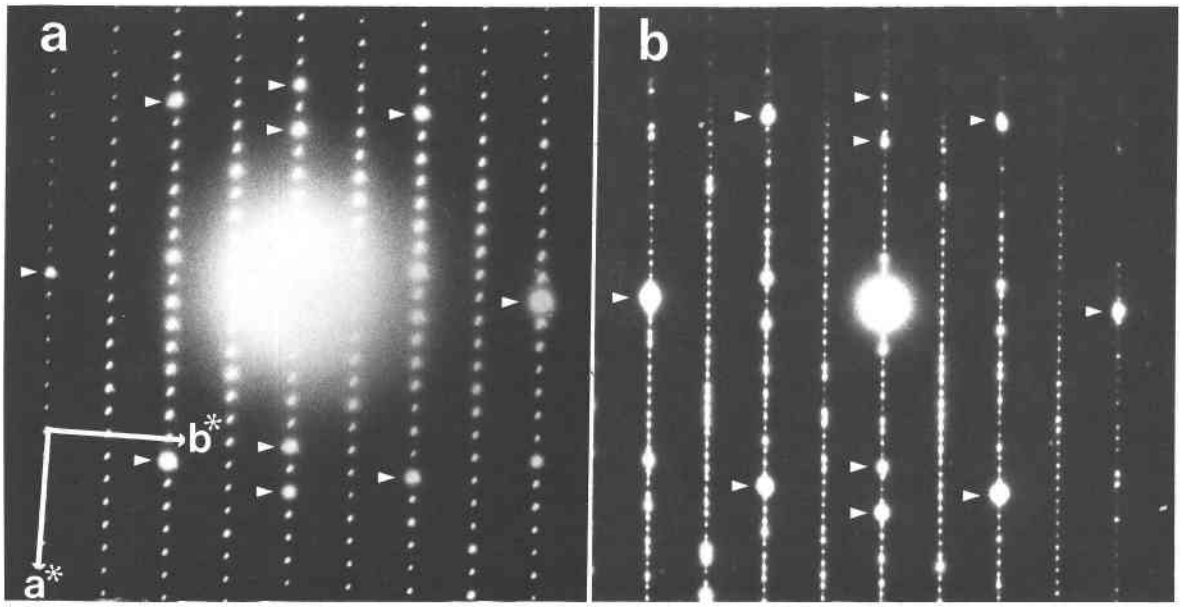

Fig. 3. Electron diffraction patterns of the baumhauerite minerals projected down [001]: (**a**) baumhauerite, (**b**) baumhauerite-*2a* (M30980). The distinctive distribution of subcell reflections is indicated in the two patterns.

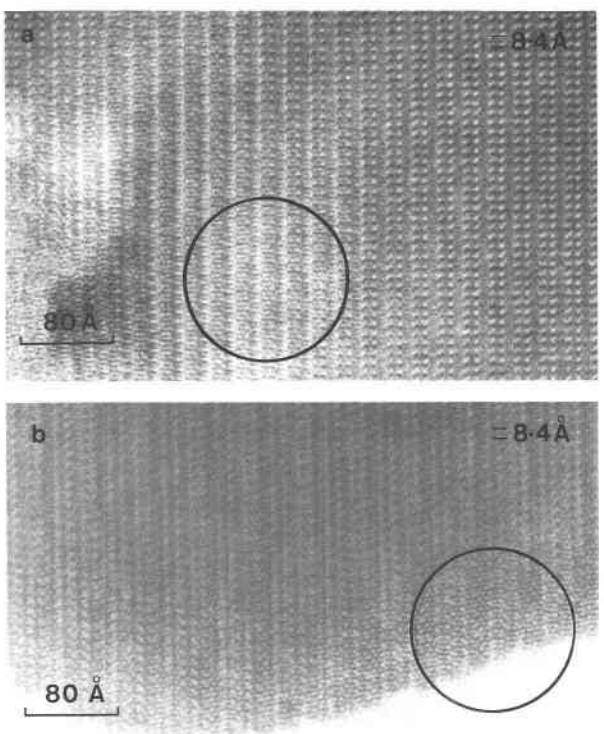

Fig. 4. High-resolution lattice images of (**a**) baumhauerite (M30980) and (**b**) baumhauerite-*2a* (M3010). Both images are projected down [001] with *a* horizontal and *b* vertical. Note that the lattice repeat of baumhauerite-*2a* is twice that of baumhauerite along **a** but equal along **b**, the 8.4 Å translation. Note also in the regions where the image detail is greatest (circled) that the lattice motifs are similar.

hauerite-*2a* is the result of chemical variation by means of cation ordering.

Discussion

Baumhauerite from Lengenbach, Switzerland, was originally described by Solly (1902) on the basis of chemical and morphological data. The original analysis gave $Pb_4As_6S_{13}$, or recalculated to 36 S atoms, $Pb_{11.1}As_{16.6}S_{36}$, an Ag-free composition, but Solly also noted an earlier analysis of "rathite" by Uhrlaub, which Solly considered to be Ag-bearing baumhauerite. Engel and Nowacki (1969) proposed $Pb_{12}As_{16}S_{36}$ as the structural formula based on their crystal-structure determination.

The structural role of Ag was considered by Engel and Nowacki, as the crystal giving rise to their intensity data had an Ag-rich composition ($Pb_{11.6}Ag_{0.6}As_{15.7}S_{36}$). They assigned Ag to partially replace As on one site and a small amount of As was found to occupy a Pb site. These substitutions, which appear to be linked, indicate that a degree of chemical variation is possible in the baumhauerite structure. This is a general feature of the Pb-As-sulfide minerals, as rathite, $Pb_3As_5S_{10}$, and dufrenoysite, $Pb_8As_8S_{20}$, have essentially the same structural framework with Pb and As atoms replacing each other, though they occupy slightly different sites (Marumo and Nowacki, 1965; Ribàr et al., 1969). The electron microprobe analyses reported here show a wide compositional range of baumhauerite-*2a* from $Pb_{10}Ag_{0.6}As_{15.8}Sb_{0.4}S_{36}$ to $Pb_{11.9}Ag_{0.7}As_{17.4}Sb_{0.5}S_{36}$. Although some of this variation may be a reflection of the uncertainties associated with electron microprobe analyses of these minerals, the analyses were performed independently in two laboratories,

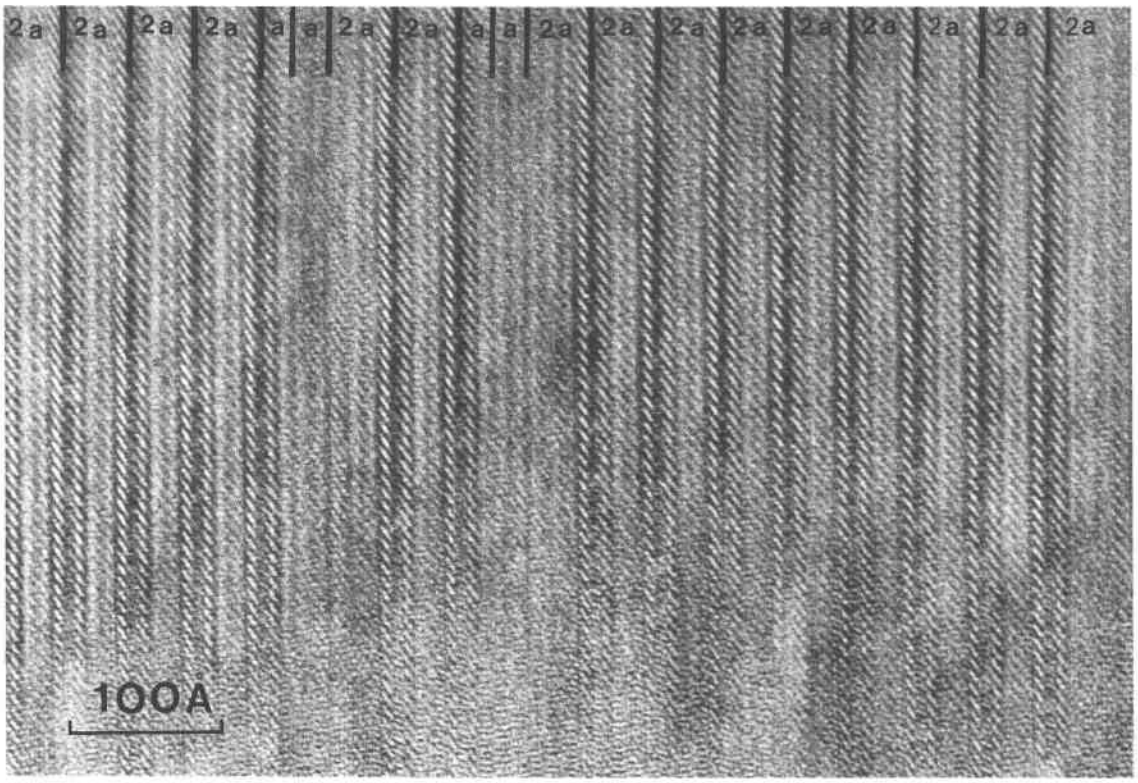

Fig. 5. High resolution image of baumhauerite-*2a* (2a) intergrown with thin strips of baumhauerite (a), [001] zone. The width of the strip of baumhauerite is 2 unit cells, and it forms a coherent intergrowth. The crystal has been slightly tilted away from the zone axis so as to highlight contrast differences between the baumhauerite-*2a* and baumhauerite units.

and the two sets of data are in good agreement. Few of the many published analyses of the Pb-As-sulfide minerals correlate closely with the formulae determined by crystal-structure analyses (see Stalder et al., 1978). The structures offer considerable flexibility to accommodate stoichiometric variation. In addition to cation substitutions, disordered structural intergrowths also occur; Pring (1990) found disordered intergrowth of sartorite-like and dufrenoysite-like structural units in a disordered liveingite. In the case of baumhauerite-*2a*, an extended compositional field is observed, and this is due to cation substitution rather than structural intergrowth. Roesch and Hellner (1959) synthesized baumhauerite and baumhauerite-*2a* (they identified this mineral as baumhauerite II) from Ag-free compositions at 280 °C and 200 atm. The results of the current study and those of Laroussi and Moelo (1988) indicate that Ag appears to be an essential component of baumhauerite-*2a*. A recent find of baumhauerite-*2a* at Quiruvilca, Peru, however, suggests that this may not be so (Robinson and Harris, 1987). The Quiruvilca material contains Tl rather than Ag, and although it may appear that the presence of monovalent cations is responsible for supercell formation, it is possible that supercell formation is due to ordering of Pb and As.

The lattice images of intergrowths show that superstructure formation results from some form of chemical ordering, the exact nature of which could not be identified from the images, but ordering of Ag, As, or Pb over the two baumhauerite cells seems most likely. A full crystal-structure analysis or more extensive and higher-resolution lattice images are required to reveal the exact nature of the cation ordering.

The literature on the minerals from the Lengenbach quarry contains many references to poorly defined minerals. In addition to rathite, also known as rathite I, there are rathite II, rathite III, and rathite IV, for all of which unit-cell parameters have been determined. Nowacki (1967) showed that liveingite and material formally known as rathite II are equivalent. The name liveingite has been adopted for this mineral, as it does not have a superstructure that is derived from the structure of rathite. It is an ordered intergrowth of dufrenoysite and sartorite-type units (Pring, 1990). Rathite IV, on the basis of cell parameters, appears to have a superstructure based on the structure of liveingite with a doubled. A mineral also identified as rathite IV, with $a = 45.9$ Å (Stalder et al., 1978) seems to be identical to baumhauerite-*2a*. Graeser's (1983) rathite 44 was examined during this study and found to be baumhauerite-*2a* and compositionally at the edge of the baumhauerite field. The so-called Ag-rich baumhauerite of Laroussi and Moelo (1988) is also baumhauerite-*2a*. A baumhauerite-like mineral from

Quiruvilca, Peru, has recently been reported (Robinson and Harris, 1987). Electron diffraction studies of this material have shown it to be baumhauerite-*2a*, possibly intergrown with baumhauerite (Pring and Robinson, unpublished data).

Further studies of the Pb-As sulfide minerals are currently underway, and it is hoped that they will clarify the mineralogical relations of this system.

Acknowledgments

We wish to thank Professor J.M. Thomas and Dr. D.A. Jefferson, who provided access to the electron microscope facilities at the Department of Physical Chemistry, University of Cambridge. The financial support (for A.P.) was provided by the Australian Research Grants Committee. The comments of B.F. Leonard and an anonymous reviewer were greatly appreciated.

References cited

Cabri, L., Criddle, A.J., La Flamme, J.H.G., Bearne, G.S., and Harris, D. (1981) Mineralogical study of complex Pt-Fe nuggets from Ethiopia. Bulletin de Minéralogie, 104, 508–525.

Criddle, A.J., Stanley, C.J., Chisholm, J.E., and Fejer, E.E. (1983) Henryite, a new copper-silver telluride from Bisbee, Arizona. Bulletin de Minéralogie, 106, 511–517.

Embrey, P.G., and Criddle, A.J. (1978) Error problems in the two media method of deriving the optical constants n and k from measured reflectances. American Mineralogist, 63, 853–862.

Engel, P., and Nowacki, W. (1969) Die Kristallstruktur von Baumhauerit. Zeitschrift für Kristallographie, 129, 178–202.

Graeser, S. (1965) Die Mineralfunde im Dolomit des Binnatales. Schweizerische Mineralogische und Petrographische Mitteilungen, 45, 597–796.

——— (1977) Famous mineral localities: Lengenbach, Switzerland. Mineralogical Record, 8, 275–281.

——— (1983) Die wissenschaftliche Bedeutung der Mineralfundstelle Lengenbach. Mineralienfreund, 1983, 84–87.

Laroussi, A., and Moelo, Y. (1988) Argent et thallium dans des sulfosels de la série de la sartorite (grisement de Lengenbach, Vallée de Binn, Suisse). Bulletin de Minéralogie (supplement), 111, 18.

Makovicky, E. (1985) The building principles and classification of sulphosalts based on the SnS archetype. Fortschritte der Mineralogie, 63, 45–89.

Marumo, F., and Nowacki, W. (1965) The crystal structure of rathite-I. Zeitschrift für Kristallographie, 122, 433–456.

Nowacki, W. (1967) Über die mögliche identität von "Liveingit" mit Rathit-II. Neues Jahrbuch für Mineralogie Monatshefte, 353–354.

Picot, P., and Johan, Z. (1982) Atlas of ore minerals, 458 p. Elsevier, Amsterdam.

Pring, A. (1990) Disordered intergrowths in lead arsenic sulfide minerals and the paragenesis of the sartorite group minerals. American Mineralogist, 75, 289–294.

Ribàr, B., Nicca, Ch., and Nowacki, W. (1969) Dreidimensionale Verfeinerung der Kristallstrukur von Dufrenoysit, $Pb_8As_8S_{20}$. Zeitschrift für Kristallographie, 130, 15–40.

Robinson, G., and Harris, D. (1987) A baumhauerite-like mineral from Quiruvilca, Peru. The Mineralogical Record, 18, 199–201.

Roesch, H., and Hellner, E. (1959) Hydrothermale Untersuchungen am System PbS-As_2S_3. Die Naturwissenschaften, 46, 72.

Scherzer, O. (1949) The theoretical resolution limit of the electron microscope. Journal of Applied Physics, 20, 20–29.

Solly, R. H. (1902) Baumhauerite, a new mineral; and Dufrenoysite. Mineralogical Magazine, 13, 151–171.

Stalder, H.A., Embrey, P., Graeser, S., and Nowacki, W. (1978) Die Mineralien des Binntales. Naturhistorisches Museum der Stadt Bern.

Manuscript received October 23, 1989
Manuscript accepted April 19, 1990